

Density Functional Theory Analyses of Nanostructures for the Delivery of 1-Aminoadamantane Antidyskinetic Drug

Mohamed J. Saadh^{1,2} , Hamit Roy^{3,*} , Egzon Ademi⁴ 

¹ Faculty of Pharmacy, Middle East University, Amman, 11831, Jordan; msaadeh@meu.edu.jo (M.J.S.); mjsaadh@yahoo.com (M.J.S.);

² Applied Science Research Center, Applied Science Private University, Amman, Jordan; msaadeh@meu.edu.jo (M.J.S.); mjsaadh@yahoo.com (M.J.S.);

³ Indian Institute of Technology, New Delhi, India; hroychem@gmail.com (H.R.);

⁴ Faculty of Natural Sciences and Mathematics, University of Tetovo, Ilinden n.n., 1200 Tetovo, Republic of North Macedonia; egzon_ademi@outlook.com (E.A.);

* Correspondence: hroychem@gmail.com (H.R.);

Scopus Author ID 57832547200

Received: 11.09.2022; Accepted: 5.11.2022; Published: 27.12.2022

Abstract: This work was performed to analyze the nanostructures for delivering a 1-aminoadamantane (ADM) antidyskinetic drug. ADM has been mainly used for the medication of dyskinesia of Parkinson's disease, besides treating some types of influenza. To this point, the drug delivery of ADM was assessed in this work with the assistance of two representative models of nanostructures, including graphene (G) and fullerene (F). In both G and F nanostructures, an iron (Fe) atom was doped to provide an active site of interactions between the ADM substance and the nanostructure. Density functional theory (DFT) calculations were performed to achieve the required results of singular and complex models. Stabilized structures and related electronic features were evaluated for the investigated model systems. Possibilities of formations for both ADM@G and ADM@F complex models were found, and the involved interactions of complexes were analyzed based on the features of the quantum theory of atoms in the molecule (QTAIM). The results indicated a higher benefit of the formation of the ADM@F complex in comparison with the formation of the ADM@G complex. Variations of levels of frontier molecular orbitals also indicated a possibility for the recognition of complex formations. Consequently, the obtained results indicated the suitability of the investigated complex models of ADM@G and ADM@F for conducting the desired drug delivery processes using appropriate nano-based surfaces as carriers.

Keywords: nanostructure; 1-aminoadamantane; antidyskinetic; influenza; DFT calculations.

© 2022 by the authors. This article is an open-access article distributed under the terms and conditions of the Creative Commons Attribution (CC BY) license (<https://creativecommons.org/licenses/by/4.0/>).

1. Introduction

The topic of drug discovery has been indeed a non-stop process for several years, and it should still be continued because of the appearance of novel diseases and infections from time to time [1-5]. Not only the new unknown diseases, but also several already known diseases do not have a certain medication, and further investigations are still required to improve the medical protocols [6-10]. In this regard, several attempts have been dedicated to enhancing drug medications by modifying their structures and combining them with other substances to approach an efficient therapeutic process [11-15]. To this point, nanostructures have been seen as useful carriers for adsorbing drug substances and conducting them up to a correct target in biological systems [16-20]. Accordingly, investigating the features of nanostructures for

employment in the delivery of specific drugs requires learning the details of such complicated processes [21-25]. To this aim, this work was performed to assess the potential of the nanostructures for the delivery of the 1-aminoadamantane (ADM) drug. ADM (Figure 1) is mainly an antidyskinetic drug for the medication of Parkinson's disease, whereas medications for some types of influenza were also reported for ADM [26, 27]. Observing drug resistance is a disadvantage of medications by ADM to be solved for a more efficient medication of this drug [28, 29].

Interestingly, the benefits of ADM for the treatment of coronavirus disease (COVID-19) were reported in recent works [30, 31]. Indeed, the new appearance of COVID-19 showed the importance of developing drug discovery concepts in both methodology and pharmaceutical substances [32-34]. To this point, enhancing the efficiency of ADM could help in approaching better treatments of diseases and infections with this already-known drug.

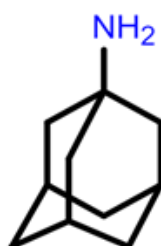


Figure 1. 1-Aminoadamantane (ADM).

As mentioned above, employing the nanostructures in combination with the drug substances could help to conduct the targeted drug delivery processes [35-38]. To this aim, two representative models of nanostructures, including graphene (G) and fullerene (F) (Figure 2), were assessed in this work for employment in the drug delivery of ADM.

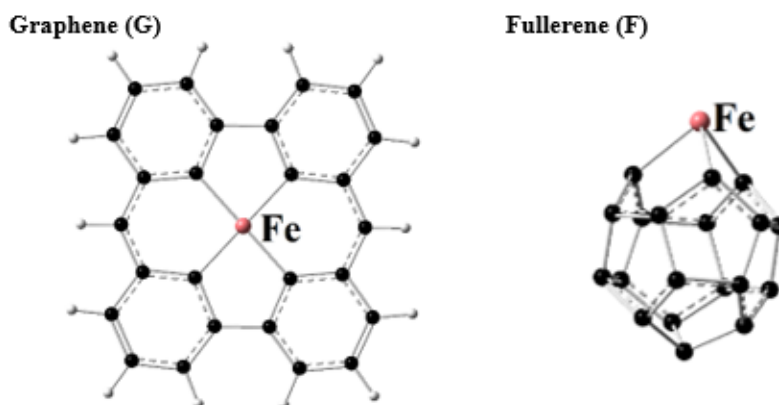


Figure 2. The Fe-doped models of graphene (G) and fullerene (F).

The electronic features of these models are exhibited in Figure 3. The results of earlier works indicated the benefits of employing both G and F nanostructures in the drug delivery processes, and they have been employed in this work accordingly [39, 40]. Additionally, an iron (Fe) atom was doped in each G and F model to provide a specified interacting site for the nanostructure interacting with the ADM drug substance. The bimolecular ADM@G and ADM@F complexes (Figure 4) were examined regarding their structural and electronic features. To obtain the required results, quantum chemical calculations were performed to optimize the structures, besides evaluating their characteristic features through the benefits of employing computational tools for dealing with complicated problems [41-45]. The singular and complex models were analyzed to assess the benefits of employing the nanostructures for

the drug delivery of ADM. Earlier works showed the need to enhance ADM features for more efficient medications [46, 47]. Accordingly, this work was performed to assess the drug delivery issue of ADM as a possible way of enhancing its efficiency for further therapeutic applications.

2. Materials and Methods

The wB97XD/6-31+G* density functional theory (DFT) calculations were performed in this work using the Gaussian program [48]. ADM, G, and F singular molecules were stabilized, and their structural and electronic features were evaluated (Figure 3). Optimization calculations were performed to obtain the stabilized structures and their related features to do this step. Electrostatic potential (ESP) surfaces, frontier molecular orbitals distribution patterns of the highest occupied molecular orbital (HOMO) and the lowest unoccupied molecular orbital (LUMO), and density of states (DOS) diagrams were evaluated for the optimized models. Next, combinations of optimized singular models were re-optimized to obtain ADM@G and ADM@F complexes (Figure 4). All interactions were examined to reach the obtained models. The interacting distances and the quantum theory of atoms in the molecule (QTAIM) features were evaluated (Table 1) for analyzing details of complex formations [49]. Moreover, energy features of both singular and complex models, including adsorption energy (EA), energies of HOMO and LUMO, and energy gap (EG), were listed in Table 2. The required features were obtained in the molecular and atomic scales by the benefits of performing computational works to provide insights into the investigated issues [50-53].

3. Results and Discussion

The nanostructure-based delivery of 1-aminoadamantane (ADM) drug was assessed in this work by performing DFT calculations. From the early detection of nanostructures, researchers have always been working on their developments for specific applications in related biological systems [54-57]. On the other hand, several unsolved therapeutic issues should be investigated to provide further insights into maintaining human health systems [58-60]. Accordingly, a possible drug delivery application was investigated within the current work by focusing on the original models of ADM and two representative nanostructures; graphene (G) and fullerene (F), as exhibited in Figures 1 and 2. The singular models were optimized to prepare the minimized energy structures for combinations in the next step. The evaluated structural and electronic features of singular models are exhibited in Figure 3. Formations of ADM@G and ADM@F were investigated by re-optimizing the bimolecular modes from the available optimized singular models, and the results are exhibited in Figure 4. To make a prediction of the interacting sites of ADM and G/F components, the results of ESP yielded a red color surface at the amine group of ADM and a blue color surface at the Fe-doped region of G and F. The mentioned colors represent the negatively charged point (red) and the positively charged point (blue). In this regard, the interacting sites were predicted to make combinations of ADM@G and ADM@F complexes. The stabilized structures of singular models and their electronic features are shown in Figure 3. As found by the DOS diagrams, a long gap distance of HOMO and LUMO was observed for the ADM component, which meant that the model could not easily participate in reaction processes with other substances. This point might stand as a reason for the occurrence of early drug resistance in the treatments by ADM. The roles of HOMO and LUMO are crucial for electron-transferring actions inside and

outside of the molecular systems, and their levels could define the chemical reactivities of the models. Indeed, HOMO and LUMO represent electron donating and accepting features of molecules by the fully occupied molecular orbital and the vacant ones to provide possibilities of such electron exchange processes. Accordingly, they could describe the tendency of molecular systems to contribute to the interaction processes. Additionally, the Fe-doped atom helped both G and F models work in interactions with the ADM substance through an assigned atomic site of the molecule. This achievement was found by the observed blue color region of ESP surfaces at the Fe-doped region of both of G and F components. Accordingly, the adsorbent models were ready for adsorbing the ADM substance through the negatively charged amine region. Next, the possibilities of the formation of such interacting complexes were examined by performing additional optimization calculations on the stabilization of bimolecular models.

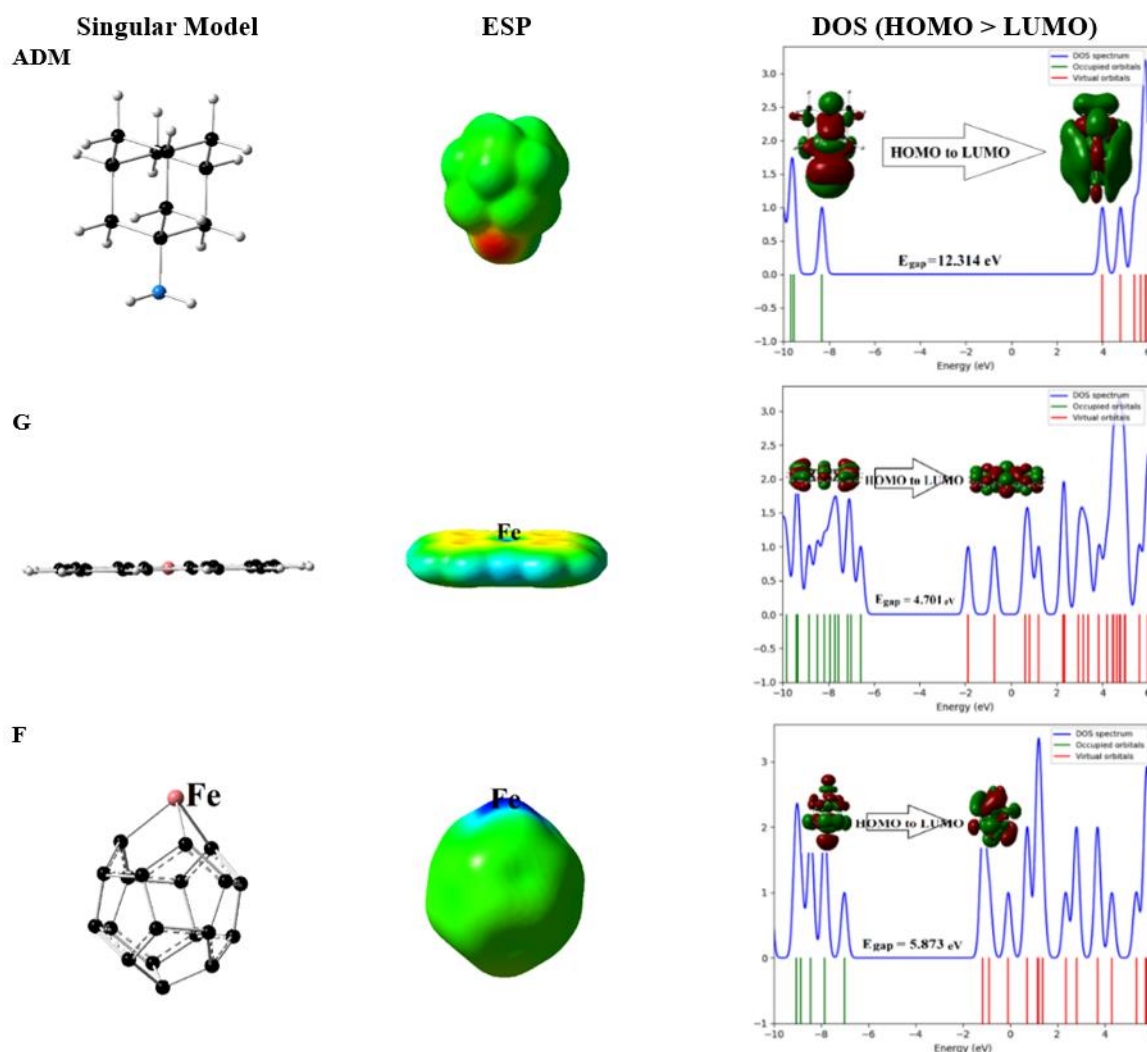


Figure 3. Structural and Electronic features of singular models.

The optimized complex models of ADM@G and ADM@F were shown in Figure 4. To learn details of interactions, the QTAIM features were evaluated (Table 1). Accordingly, the configuration of interacting models was found by the evaluated QTAIM features showing existence of three interactions for formations of each of ADM@G and ADM@F complex models. H...C and N...F are two types of interactions of ADM@G complex and C...Fe, N...Fe, and H...C are three types of interactions of ADM@F complex. The interaction details and strengths of complexes were found based on the obtained QTAIM results. A type of semi-

hydrogen-bond interaction was observed in both complexes with a noticeable strength by the evaluated QTAIM values (Table 1). The N atom of ADM interacted with the Fe-doped atom in the stabilized ADM@G complex, whereas the C and N atoms were involved in interactions in the stabilized ADM@F complex. The spherical structure of F may provide a more suitable surface for the relaxation of ADM substance during the optimization process in comparison with the G model, as the ADM substance was relaxed closer to the F surface than the G surface. The magnitudes and signs of ρ , $\nabla^2\rho$, and H showed that two H...C interactions of ADM@G were weak interactions, and one N...Fe interaction was strong. One H...C interaction of ADM@F was a weak interaction and C...Fe and N...Fe interactions were strong. Accordingly, the adsorption process of ADM by the F model was more suitable than the G model.

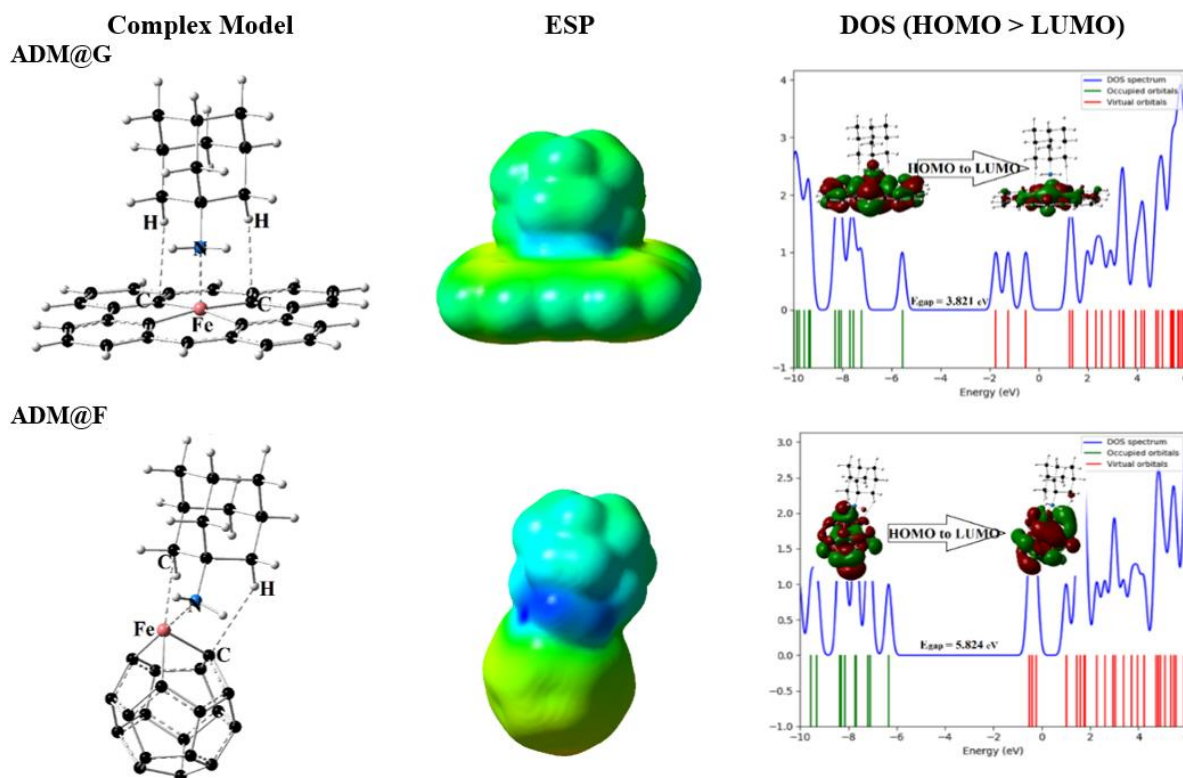


Figure 4. Structural and Electronic features of complex models.

Table 1. QTAIM features of complex models.*

Feature	ADM@G			ADM@F		
	H...C	N...Fe	H...C	C...Fe	N...Fe	H...C
Int						
D Å	2.45	2.06	2.52	2.53	1.99	2.66
ρ au	0.01	0.08	0.01	0.03	0.09	0.01
$\nabla^2\rho$ au	0.04	-0.33	0.04	-0.11	-0.48	0.03
H au	0.01	-0.01	0.01	-0.01	-0.02	0.01

*The models are exhibited in Figure 4. Int: interaction, D; distance, ρ : total electron density, $\nabla^2\rho$: Laplacian of electron density, H: energy density.

Based on the obtained energy features of Table 2, the formation of the ADM@F complex was found more suitable than that of the ADM@G complex regarding the evaluated values of E_A of -46.34 kcal/mol and -32.22 kcal/mol, respectively. In this regard, the evaluated QTAIM features and E_A values indicated the strength levels of complex formations for the optimized bimolecular models. It should be noted that the adsorption of ADM by both of G and F adsorbents was almost affirmed with higher suitability for the formation of ADM@F complex than ADM@G complex. For further analyses of the models, energy levels of HOMO and LUMO were included in Table 2. The original wide gap of singular ADM

($E_G=12.31$ eV) came closer to 3.82 and 5.82 eV in ADM@G and ADM@F complexes, respectively. To interpret such observed variations, each of the original HOMO and LUMO levels was migrated to new levels. Localizations of both HOMO and LUMO distribution patterns were placed at the surfaces of G and F counterparts in both complexes to show the protective role of nanostructures for conducting the targeted drug delivery purposes up to a correct destination. Additionally, variations of DOS diagrams and E_G values among the models showed a possibility of sensing the process of the models in singular and complex states.

Table 2. Energy features of singular and complex models.*

Feature	ADM	G	F	ADM@G	ADM@F
E_A kcal/mol	n/a	n/a	n/a	-32.22	-46.34
HOMO eV	-8.32	-6.58	-7.02	-5.56	-6.34
LUMO eV	3.99	-1.88	-1.15	-1.74	-0.51
E_G eV	12.31	4.70	5.87	3.82	5.82

*The models are exhibited in Figures 1-4. E_A : adsorption energy, HOMO: energy of the highest occupied molecular orbital, LUMO: energy of the lowest unoccupied molecular orbital, E_G : energy gap of HOMO and LUMO levels.

4. Conclusions

The benefits of formations of ADM@G and ADM@F complexes for conducting the ADM drug delivery were found. The optimization calculations obtained the stabilized structures, and the related electronic features showed characteristic variations for the models. The formation of both ADM@G and ADM@F complexes were affirmed based on the QTAIM and energy features with higher suitability for the ADM@F complex. A type of H...C semi-hydrogen-bond interaction was recognized in both complexes. A possibility of reorganizing the investigated models in singular and complex states was found by the results of HOMO and LUMO frontier molecular orbitals and their distance gap, revealing a sensor function for the investigated singular and complex models. Finally, the investigated ADM@G and ADM@F complexes were suitable for conducting the ADM drug delivery process.

Funding

This research received no external funding.

Acknowledgments

This research has no acknowledgment.

Conflicts of Interest

The authors declare no conflict of interest.

References

1. Mouchlis, V.D.; Afantitis, A.; Serra, A.; Fratello, M.; Papadiamantis, A.G.; Aidinis, V.; Lynch, I.; Greco, D.; Melagraki, G. Advances in de novo drug design: from conventional to machine learning methods. *International Journal of Molecular Sciences* **2021**, *22*, 1676, <https://doi.org/10.3390/ijms22041676>.
2. Medina-Franco, J.L. Grand challenges of computer-aided drug design: the road ahead. *Frontiers in Drug Discovery* **2021**, *1*, 728551, <https://www.frontiersin.org/articles/10.3389/fddsv.2021.728551/full>.
3. Mehrabian, M.; Ahari, U.Z.; Fathi, A.; Parizi, M.M. Comparison of dental health status in schizophrenic patients with healthy individuals. *Clinical Schizophrenia & Related Psychoses* **2021**, *15*, 5, <https://doi.org/10.3371/CSRP.MMUA.102821>.

4. Jalali Kondori, B.; Hemadi, S.; Esmaeili Gouvarchin Ghaleh, H.; Milani Fard, A.; Dorostkar, R. Pharmacological study of the antitumor effect of newcastle oncolytic virus in combination with copper nanoparticles, hyperthermia and radiation on malignant colorectal cancer cell line. *Journal of Medicinal and Chemical Sciences* **2022**, *5*, 457-467, <https://doi.org/10.26655/jmchemsci.2022.4.2>.
5. Nazneen A. Scrotal defects reconstruction after Fournier's gangrene. *International Journal of Scientific Research in Dental and Medical Sciences* **2021**, *3*, 184, <https://doi.org/10.30485/ijrdms.2021.315745.1217>.
6. Olaleye, O.; Oladipupo, A.; Oyawaluja, B.; Coker, H. Chemical composition, antioxidative and antimicrobial activities of different extracts of the leaves of *parquetina nigrescens* (asclepiadaceae). *Progress in Chemical and Biochemical Research* **2021**, *4*, 359-371, <https://doi.org/10.22034/pcbr.2021.287025.1188>.
7. Ghasemi, E.; Fathi, A.H.; Parvizinia, S. Effect of three disinfectants on dimensional changes of different impression materials. *Journal of Iranian Dental Association* **2019**, *31*, 169-176, <https://doi.org/10.30699/jidai.31.3.169>.
8. Nopour, R.; Mashoufi, M.; Amraei, M.; Mehrabi, N.; Mohammadnia, A.; Mahdavi, A.; Mirani, N.; Saki, M.; Shanbehzadeh, M. Performance analysis of selected decision tree algorithms for predicting drug adverse reaction among COVID-19 hospitalized patients. *Journal of Medicinal and Chemical Sciences* **2022**, *5*, 505-517, <https://doi.org/10.26655/jmchemsci.2022.4.7>.
9. Abolhasani, M.; Ghasemi, E.; Fathi, A.H.; Hayatizadeh, M.J. Color change of ceramill zolid fx following abrasion with/without toothpaste. *Journal of Iranian Dental Association* **2021**, *33*, 51-57, <https://doi.org/10.52547/jida.33.3.4.51>.
10. Fathi, A.; Ebadian, B.; Dezaki, S.N.; Mardasi, N.; Mosharraf, R.; Isler, S.; Tabatabaei, S.S. An umbrella review of eystematic reviews and meta-qnalyzes evaluating the success rate of prosthetic restorations on endodontically treated teeth. *International Journal of Dentistry* **2022**, *2022*, 4748291, <https://doi.org/10.1155/2022/4748291>.
11. Al Samarrai, E.; Alwan, L.; Al-Haddad, S.; Al Samarrai, M.; Al-Obaidi, M.; Al Samarrai, O. Spectrophotometric determination of phenobarbital in pharmaceutical preparation using gold nanoparticles. *Eurasian Chemical Communications* **2022**, *4*, 812, <https://doi.org/10.22034/ecc.2022.329806.1329>.
12. Ulası, T.; Nri-Ezedi, C.; Ofiaeli, O.; Chijioke, E. Novel cases of diamond blackfan anaemia in two Nigerian toddlers: roadmap for care in resource-limited nations. *International Journal of Scientific Research in Dental and Medical Sciences* **2021**, *3*, 101, <https://doi.org/10.30485/ijrdms.2021.282666.1148>.
13. Jasim, S.; Mustafa, Y. Synthesis, ADME study, and antimicrobial evaluation of novel naphthalene-based Derivatives. *Journal of Medicinal and Chemical Sciences* **2022**, *5*, 793-807, <https://doi.org/10.26655/jmchemsci.2022.5.14>.
14. Maalekipour, M.; Safari, M.; Barekatin, M.; Fathi, A. Effect of adhesive resin as a modeling liquid on elution of resin composite restorations. *International Journal of Dentistry* **2021**, *2021*, 3178536, <https://doi.org/10.1155/2021/3178536>.
15. N'Guessan, D.; Coulibaly, S.; Kassi, F.; Delaye, P.; Penichon, M.; Enguehard-Gueiffier, C.; Allouchi, H.; Ouattara, M. Synthesis and SAR of imidazo[1,2-a] pyridinyl-phenylacrylonitrile derivatives as potent anticandidosis agents. *Journal of Medicinal and Chemical Sciences* **2021**, *4*, 554-563, <https://doi.org/10.26655/jmchemsci.2021.6.3>.
16. Hatami, A.; Heydarinasab, A.; Akbarzadehkhayavi, A.; Pajoum Shariati, F. An introduction to nanotechnology and drug delivery. *Chemical Methodologies* **2021**, *5*, 153, <https://doi.org/10.22034/chemm.2021.121496>.
17. Baghernejad, B.; Alikhani, M. Nano-cerium oxide/aluminum oxide as an efficient catalyst for the synthesis of xanthene derivatives as potential antiviral and anti-inflammatory agents. *Journal of Applied Organometallic Chemistry* **2022**, *2*, 155-162, <https://doi.org/10.22034/jaoc.2022.154819>.
18. Mahmoud, J.; Ghareeb, O.; Mahmood, Y. The role of garlic oil in improving disturbances in blood parameters caused by zinc oxide nanoparticles. *Journal of Medicinal and Chemical Sciences* **2022**, *5*, 76-81, <https://doi.org/10.26655/jmchemsci.2022.1.9>.
19. Baghernejad, B. Preparation of polyhydroquinolines in the presence of nano cerium (IV)oxide/zinc oxide as an efficient catalyst. *Journal of Applied Organometallic Chemistry* **2022**, *2*, 74-80, <https://doi.org/10.22034/jaoc.2022.340645.1054>.
20. Shete, R.; Fernandes, P.; Borhade, B.; Pawar, A.; Sonawane, M.; warude, N. Review of cobalt oxide nanoparticles: green synthesis, biomedical applications, and toxicity studies. *Journal of Chemical Reviews* **2022**, *4*, 331-345, <https://doi.org/10.22034/jcr.2022.342398.1172>.

21. Hosseini, S.; Naimi-Jamal, M.; Hassani, M. Preparation and characterization of mebeverine hydrochloride niosomes as controlled release drug delivery system. *Chemical Methodologies* **2022**, *6*, 591, <https://doi.org/10.22034/chemm.2022.337717.1482>.
22. Sheikholeslami-Farahani, F. Amine functionalized SiO₂@Fe₃O₄ as a green and reusable magnetic nanoparticles system for the synthesis of Knoevenagel condensation in water. *Asian Journal of Nanosciences and Materials* **2022**, *5*, 132-143, <https://doi.org/10.26655/ajnanomat.2022.2.5>.
23. Hatami, A. Preparation, description and evaluation of the lethality acid loaded liposomal nanoparticles against in vitro colon and liver cancer. *Journal of Chemical Reviews* **2021**, *3*, 121-133, <https://doi.org/10.22034/jcr.2021.283609.1109>.
24. Patel, K.; Chandankar, S.; Mahajan, H. Synthesis and characterization of curcumin nanoparticles by hydrothermal method. *Asian Journal of Nanosciences and Materials* **2021**, *4*, 321-330, <https://doi.org/10.26655/AJNANOMAT.2021.4.7>.
25. Zaid Almarbd, Z.; Mutter Abbass, N. Synthesis and characterization of TiO₂, Ag₂O, and graphene oxide nanoparticles with polystyrene as a nanocomposites and some of their applications. *Eurasian Chemical Communications* **2022**, *4*, 1033, <https://doi.org/10.22034/ecc.2022.342801.1469>.
26. Pham, V.H.; Tran, T.H.; Vu, B.D.; Le, H.B.; Nguyen, H.T.; Phan, D.C. A simple process for the synthesis of 1-aminoadamantane hydrochloride. *Organic Preparations and Procedures International* **2020**, *52*, 77, <https://doi.org/10.1080/00304948.2019.1697618>.
27. Perez-Lloret, S.; Rascol, O. Efficacy and safety of amantadine for the treatment of L-DOPA-induced dyskinesia. *Journal of Neural Transmission* **2018**, *125*, 1237, <https://doi.org/10.1007/s00702-018-1869-1>.
28. Wang, L.Y.; Zhao, M.Y.; Bu, F.Z.; Niu, Y.Y.; Yu, Y.M.; Li, Y.T.; Yan, C.W.; Wu, Z.Y. Cocrystallization of amantadine hydrochloride with resveratrol: the first drug–nutraceutical cocrystal displaying synergistic antiviral activity. *Crystal Growth & Design* **2021**, *21*, 2763, <https://doi.org/10.1021/acs.cgd.0c01673>.
29. Bode, L.; Dietrich, D.E.; Spannhuth, C.W.; Ludwig, H. Prominent efficacy of amantadine against human borna disease virus infection in vitro and in vivo. *Viruses* **2022**, *14*, 494, <https://doi.org/10.3390/v14030494>.
30. Cortés-Borra, A.; Aranda-Abreu, G.E. Amantadine in the prevention of clinical symptoms caused by SARS-CoV-2. *Pharmacological Reports* **2021**, *73*, 962, <https://doi.org/10.1007/s43440-021-00231-5>.
31. Rejdak, K.; Grieb, P. Fluvoxamine and amantadine: central nervous system acting drugs repositioned for COVID-19 as early intervention. *Current Neuropharmacology* **2022**, *20*, 777, <https://doi.org/10.2174/1570159x19666210729123734>.
32. Singh, A.; Brar, R.; Virk, A.; Verma, S.K. The impact of metabolic syndrome on clinical outcome of COVID-19 patients: a retrospective study. *International Journal of Scientific Research in Dental and Medical Sciences* **2021**, *3*, 161, <https://doi.org/10.30485/ijrdms.2021.307324.1201>.
33. Kausikan, S.P.; Anu, S.; Saravanan, M.; Devisri, T.; Rekha, K.; John, R. The impact of COVID-19 on auditory and visual choice reaction time of non-hospitalized patients: an observational study. *International Journal of Scientific Research in Dental and Medical Sciences* **2022**, *4*, 21, <https://doi.org/10.30485/ijrdms.2022.327884.1250>.
34. Munagala, S.; Rachamadugu, H.; Avileli, S.; Avula, R.; Beladona, N.J.; Boyapally, S.R. Microbiological profile of post-COVID-19 mucormycosis in various samples. *International Journal of Scientific Research in Dental and Medical Sciences* **2022**, *4*, 87, <https://doi.org/10.30485/ijrdms.2022.338567.1285>.
35. Alinezhad, H.; Hajiabbas Tabar Amiri, P.; Mohseni Tavakkoli, S.; Muhiebes, R.; Fakri Mustafa, Y. Progressive types of Fe₃O₄ nanoparticles and their hybrids as catalysts. *Journal of Chemical Reviews* **2022**, *4*, 288-312, <https://doi.org/10.22034/jcr.2022.325255.1137>.
36. Yaraghi, A.; Ozkendir, O.M.; Mirzaei, M. DFT studies of 5-fluorouracil tautomers on a silicon graphene nanosheet. *Superlattices and Microstructures* **2015**, *85*, 784, <https://doi.org/10.1016/j.spmi.2015.05.053>.
37. Alizadeh, S.; Nazari, Z. Amphetamine, methamphetamine, morphine @AuNPs kit based on PARAFAC. *Advanced Journal of Chemistry-Section A* **2022**, *5*, 253-262, <https://doi.org/10.22034/ajca.2022.345350.1318>.
38. Mirzaei, M.; Hadipour, N.; Gulseren, O. DNA codon recognition by a cubane wire: in silico approach. *Turkish Computational and Theoretical Chemistry* **2021**, *5*, 13-119, <https://doi.org/10.33435/tcandtc.828634>.
39. Ali Fadhil, H.; H. Samir, A.; Abdulghafoor Mohammed, Y.; Al. Rubaei, Z.M.M. Synthesis, characterization, and in vitro study of novel modified reduced graphene oxide (RGO) containing heterocyclic compounds as anti-breast cancer. *Eurasian Chemical Communications* **2022**, *4*, 1156, <https://doi.org/10.22034/ecc.2022.345188.1484>.

40. Golipour-Chobar, E.; Salimi, F.; Ebrahimzadeh-Rajaei, G. Sensing of lomustine drug by pure and doped C48 nanoclusters: DFT calculations. *Chemical Methodologies* **2022**, *6*, 790, <https://doi.org/10.22034/chemm.2022.344895.1555>.
41. Oyenyin, O.; Abayomi, T.; Ipinloju, N.; Agbaffa, E.; Akerele, D.; Arobadade, O. Investigation of amino chalcone derivatives as anti-proliferative agents against MCF-7 breast cancer cell lines-DFT, molecular docking and pharmacokinetics studies. *Advanced Journal of Chemistry-Section A* **2021**, *4*, 288-299, <https://doi.org/10.22034/ajca.2021.285869.1261>.
42. Tandon, H.; Chakraborty, T.; Suhag, V. A brief review on importance of DFT in drug design. *Research in Medical and Engineering Studies* **2019**, *7*, RMES.000668, <https://crimsonpublishers.com/rmes/pdf/RMES.000668.pdf>.
43. Venkatesh, G.; Sheena Mary, Y.; Shymamary, Y.; Palanisamy, V.; Govindaraju, M. Quantum chemical and molecular docking studies of some phenothiazine derivatives. *Journal of Applied Organometallic Chemistry* **2021**, *1*, 148-158, <https://doi.org/10.22034/jaoc.2021.303059.1033>.
44. Hosouna, B.; Malek, H.; Abdelsalam, S.M.; Ahwidy, Z. Computational study of the effectiveness of natural herbal derivatives on COVID-19 virus. *Advanced Journal of Chemistry-Section B* **2021**, *3*, 323-332, <https://doi.org/10.22034/ajcb.2021.305568.1094>.
45. Saravanamoorthy, S.; Banu, M.; Rachel Joy, R. Computational analysis and molecular docking study of 4-(carboxyamino)-3-guanidino-benzoic acid. *Advanced Journal of Chemistry-Section B* **2021**, *3*, 120-147, <https://doi.org/10.22034/ajcb.2021.260742.1072>.
46. Gmiro, V.E.; Zhigulin, A.S. Search for selective GluA1 ampa antagonists in a series of dicationic compounds. *Pharmaceutical Chemistry Journal* **2022**, *56*, 309, <https://doi.org/10.1007/s11094-022-02635-w>.
47. Mohamed, M.S.; El Sayed, I.; Zaki, A.; Abdelmonem, S. Assessment of the effect of amantadine in patients with traumatic brain injury: a meta-analysis. *Journal of Trauma and Acute Care Surgery* **2022**, *92*, 605, <https://doi.org/10.1097/TA.0000000000003363>.
48. Frisch, M.J.; Trucks, G.W.; Schlegel, H.B. et al. Gaussian 09 program. *Gaussian Inc.* **2009**, Wallingford, CT.
49. Cortés-Guzmán, F.; Bader, R.F. Complementarity of QTAIM and MO theory in the study of bonding in donor-acceptor complexes. *Coordination Chemistry Reviews* **2005**, *249*, 633, <https://doi.org/10.1016/j.ccr.2004.08.022>.
50. Sharma, R.; Singh, M.; Kamal, K.; Ghatpande, N.; Shaikh, M.; Jadhav, J.; Murugavel, S.; Kant, R. Synthesis, crystal structure, Hirshfeld surface, crystal voids, energy frameworks, DFT and molecular docking analysis of (2,6-dimethoxyphenyl)acetic acid. *Advanced Journal of Chemistry-Section B* **2022**, *4*, 1-16, <https://doi.org/10.22034/ajcb.2022.320258.1102>.
51. Darougari, H.; Rezaei-Sameti, M. The drug delivery appraisal of Cu and Ni decorated B12N12 nanocage for an 8-hydroxyquinoline drug: A DFT and TD-DFT computational study. *Asian Journal of Nanosciences and Materials* **2022**, *5*, 196-210, <https://doi.org/10.26655/AJNANOMAT.2022.3.3>.
52. Ameji, J.; Uzairu, A.; Shallangwa, A.; Uba, S. Molecular docking study and insilico design of novel drug candidates against salmonella typhi. *Advanced Journal of Chemistry-Section B* **2022**, *4*, 281-298, <https://doi.org/10.22034/ajcb.2022.366678.1129>.
53. Shinde, R.; Adole, V. Anti-microbial evaluation, experimental and theoretical insights into molecular structure, electronic properties, and chemical reactivity of (E)-2-((1H-indol-3-yl)methylene)-2,3-dihydro-1H-inden-1-one. *Journal of Applied Organometallic Chemistry* **2021**, *1*, 48-58, <https://doi.org/10.22034/jaoc.2021.278742.1011>.
54. Mortezagholi, B.; Movahed, E.; Fathi, A.; Soleimani, M.; Forutan Mirhosseini, A.; Zeini, N.; Khatami, M.; Naderifar, M.; Abedi Kiasari, B.; Zareanshahraki, M. Plant-mediated synthesis of silver-doped zinc oxide nanoparticles and evaluation of their antimicrobial activity against bacteria cause tooth decay. *Microscopy Research and Technique* **2022**, *85*, 3553-3564, <https://doi.org/10.1002/jemt.24207>.
55. Jassim, L.; Mahmood, K. Study of some physicochemical, microbial and sensory properties of low-fat butter produced by titanium dioxide (TiO₂) nano particles. *Eurasian Chemical Communications* **2022**, *4*, 241-255, <https://doi.org/10.22034/ecc.2022.318882.1275>.
56. Aminian, A.; Fathi, A.; Gerami, M.H.; Arsan, M.; Forutan Mirhosseini, A.; Torabzadeh, S.A. Nanoparticles to overcome bacterial resistance in orthopedic and dental implants. *Nanomedicine Research Journal* **2022**, *7*, 107-123, <https://doi.org/10.22034/nmrj.2022.02.001>.
57. Hosseini, S.A.; Shojaie, F.; Afzali, D. Analysis of structural, and electronic properties of clopidogrel drug adsorption on armchair (5, 5) Single-walled carbon nanotube. *Asian Journal of Nanosciences and Materials* **2021**, *4*, 15-30, <https://doi.org/10.26655/AJNANOMAT.2021.1.2>.

58. Khosravian, M.; Momenzadeh, M.; Koosha, F.; Alimohammadi, N.; Kianpour, N. Lung cancer risk and the inhibitors of angiotensin converting enzyme; an updated review on recent evidence. *Immunopathologia Persa* **2022**, *8*, e19, <https://doi.org/10.34172/ipp.2022.19>.
59. Hiawi, F.A.; Ali, I.H. Study the adsorption behavior of food colorant dye indigo carmine and loratadine drug in solution. *Chemical Methodologies* **2022**, *6*, 720-730, <https://doi.org/10.22034/chemm.2022.349806.1570>.
60. Asgharpour, M.; Kalan, M.E.; Mirhashemi, S.H.; Alirezaei, A. Lung cancer risk and the inhibitors of angiotensin converting enzyme: a mini-review of recent evidence. *Immunopathologia Persa* **2019**, *5*, e16, <https://doi.org/10.15171/ipp.2019.16>.